Supporting Information:

Structure-Function Relationships in Single-Molecule Rectification by *N*-phenylbenzamide Derivatives

Christopher Koenigsmann,[a,b†] *Wendu Ding,*[a, c,†] *Matthieu Koepf,*[a] *Arunabh Batra,*[d] *Latha Venkataraman,*[d,*] *Christian F. A. Negre,*[a,b,e*] *Gary W. Brudvig,*[a,c,*] *Robert H. Crabtree.*[a,c,*] *Victor S. Batista,*[a,c,*] and *Charles A. Schmuttenmaer*[a,c,*]

[a] Yale Energy Sciences Institute, Yale University, P.O. Box 27394, West Haven, CT 06516-7394, USA.

[b] Department of Chemistry, Fordham University, 441 East Fordham Road, Bronx, NY 10458, USA.

[c] Department of Chemistry, Yale University, P.O. Box 208107, New Haven, CT 06520-8107, USA.

[d] Department of Applied Physics and Applied Mathematics, Columbia University, New York, NY 10027, USA.

[e] Theoretical Division, Los Alamos National Laboratory, P.O. Box 1663, Los Alamos, New Mexico, 87545, USA.

† These authors contributed equally to this work.

Table of Contents

Synthesis of Rectifier Molecules

Reagents, solvents and general glassware handling used for synthesis:

4-[(*tert*-butoxycarbonyl)amino]benzoic acid, 4-[(*tert*-butoxycarbonyl)amino]aniline, 4-nitrobenzoyl chloride, *N*-methyl-4-nitroaniline, *N*-ispropyl-4-nitroaniline, *N,N*-diisopropylethylamine (DIPEA), trifluoroacetic acid (TFA), and hydrazine monohydrate (reagent purities: 97% or higher) were obtained from Alfa Aesar. 1-Ethyl-3-(3-dimethylaminopropyl)carbodiimide (EDCI) (97%) was purchased from Bachem. 4-(*N,N*-dimethylamino)pyridine (DMAP), and 4-nitro-2,5-dimethoxyaniline, (reagent purities:97% or higher) were obtained from Acros Organics. 5%-palladium on carbon (Evonik E-101 E R/W 5%) was purchased from Strem Chemicals. All the reagents were used as received. For synthetic purposes dichloromethane (CH_2Cl_2, OmniSolv grade, EMD-Millipore) and tetrahydrofuran (THF, OmniSolv grade, non stabilized, EMD-Millipore) were dried on a Pure Solv MD-5 solvent purification system (Innovative Technology) on activated aluminum oxide before use and were dispensed under nitrogen. 200 proof ethanol (EtOH, Decon labs), and chloroform ($CHCl_3$, ACS grade, stabilized with amylenes, BDH) were used as received. *N.N*-Diisopropylethylamine (DIPEA) was freshly distilled over potassium hydroxide (KOH) and stored under argon (Ar). The glassware was oven-dried and cooled under nitrogen prior to use. Anhydrous sodium sulfate (Na_2SO_4), sodium bicarbonate ($NaHCO_3$), citric acid, and sodium chloride (ACS grade) were obtained from JT-Baker. For purification purposes, dichloromethane (ACS grade, stabilized with amylenes, BDH), chloroform (ACS grade, stabilized with amylenes, BDH) ethyl acetate (EtOAc, ACS grade, BDH), and toluene (ACS grade, Macron Fine Chemicals) were used without further purification. For nuclear magnetic resonance studies (NMR), deuterated dimethylsulfoxide (DMSO-d_6 containing 0.05% v/v of tetramethylsilane (TMS)) and deuterated chloroform ($CDCl_3$, containing 0.05% v/v TMS) were obtained from Cambridge Isotope Laboratory. Analytical thin layer chromatography (TLC) was conducted on glass-coated silica gel 60 F254 plates obtained from EMD-Millipore. Column chromatography was conducted on silica gel (SiO_2, 43–60 μm) provided by Silicycle. Celite 545 was purchased from EMD-Millipore. NMR spectra were recorded on a Varian DPX spectrometer coupled to an Oxford 400 magnet. ^1H spectra were recorded at 400 MHz, and ^{13}C NMR at 101 MHz. Chemical shifts are reported versus tetramethylsilane as internal reference. Mass spectrometry was performed on an Agilent G6550A Q-TOF LC/MS with API by direct injection, the compounds were dissolved in methanol at an approximate concentration of 0.5 mg/mL. All the synthesized N-phenylbenzamide derivatives were stored under Ar at -20°C.

Experimental procedures:

4-[(*tert*-butoxycarbonyl)amino]-*N*-[4-(*tert*-butoxycarbonyl)aminophenyl]benzamide

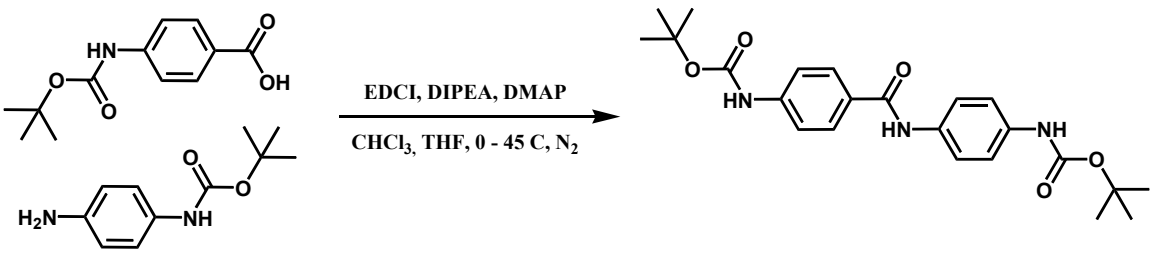

4-[(*tert*-butoxycarbonyl)amino]benzoic acid (500 mg, 2.11 mmol) was dissolved in a 1:1 mixture of THF and chloroform (50 mL), *N,N*-diisopropylethylamine (1 mL, 0.747 g, 5.8 mmol) was added and the solution was cooled to 0 °C under nitrogen. 1-Ethyl-3-(3-dimethylaminopropyl)carbodiimide (460 mg, 2.4 mmol, 1.14 eq) was added and the mixture was stirred at 0 °C for 30 minutes. 4-[(*tert*-

butoxycarbonyl)amino]-aniline (440 mg, 2.11 mmol, 1eq) was added and the mixture stirred at 0 °C under nitrogen for 30 minutes before being slowly warmed to 45 °C. The progression of the reaction was followed by TLC analysis (SiO_2, CH_2Cl_2: 20%-EtOAc). After stirring 2 hours at 45 °C a large amount of solid precipitated and only trace amounts of staring material were detected by TLC; the mixture was cooled to room temperature, and diluted to 100 mL with dichloromethane. The suspension was successively extracted with 5% aqueous $NaHCO_3$ (2 × 100 mL), 5% citric acid (2 × 100 mL) and water (2 × 100 mL). The organic layer was collected and the solvent was evaporated. The crude solid was suspended in toluene (25 mL) and the solvent evaporated. This treatment was repeated two times to eliminate the remaining water. Due to the poor solubility of the resulting material, it was immediately used in the next reaction without further purification. Yield 587 mg (1.37 mmol, 65%), off-white solid, estimated purity by NMR ~90%.
^{1}H-NMR (400 MHz, DMSO-d_6) δ (ppm): 9.92 (s, 1H), 9.62 (s, 1H), 9.23 (s, 1H), 7.84 (d, J = 8.8 Hz, 2H), 7.58 (d, J = 9.0 Hz, 2H), 7.53 (d, J = 8.8 Hz, 2H), 7.36 (d, J = 8.8 Hz, 2H), 1.44 (s, 9H).

4-amino-*N*-(4-aminophenyl)benzamide

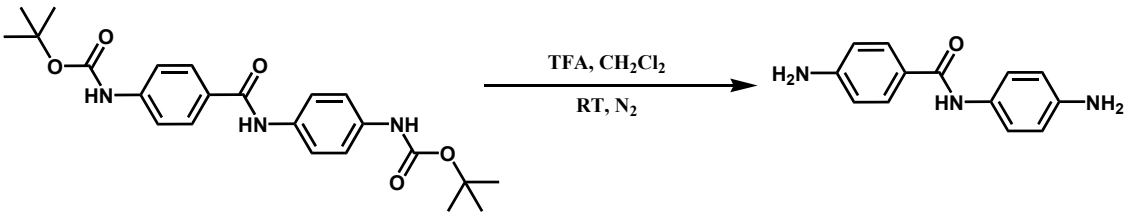

The crude 4-[(*tert*-butoxycarbonyl)amino]-*N*-[4-(*tert*-butoxycarbonyl)aminophenyl] benzamide (450 mg, 1.05 mmol) was suspended in dichloromethane (50 mL) and trifluoroacetic acid (10 mL) added. The mixture was then stirred at room temperature. After 2 hours the solid was fully dissolved and TLC analysis (SiO_2, CH_2Cl_2:10%-EtOAc) showed that the reaction was complete. The mixture was diluted to 100 mL with dichloromethane and successively washed with a 5% aqueous $NaHCO_3$ solution (3 × 100 mL) then water (2 × 100 mL). The organic layer was collected, dried over Na_2SO_4, filtered, and the solvent was evaporated. Column chromatography (SiO_2, CH_2Cl_2: 10%-EtOAc) yielded the desired compound as an off-white solid (175 mg, 0.77 mmol, 73%).
^{1}H-NMR (400 MHz, DMSO-d_6) δ (ppm): 9.36 (s, 1H), 7.64 (d, J = 8.6 Hz, 2H), 7.30 (d, J = 8.7 Hz, 2H), 6.55 (d, J = 8.6 Hz, 2H), 6.50 (d, J = 8.7 Hz, 2H), 5.61 (brs, 2H), 4.84 (brs, 2H).
^{13}C-NMR (101 MHz, DMSO-d_6) δ (ppm): 165.01, 152.07, 145.05, 129.41, 129.19, 122.54, 122.11, 114.09, 112.95.
HRMAS (m/z): calc for $C_{13}H_{13}N_3O+H^+$, 228.11314; found, 228.11302

***N*-methyl-4-nitro-*N*-(4-nitrophenyl)benzamide**

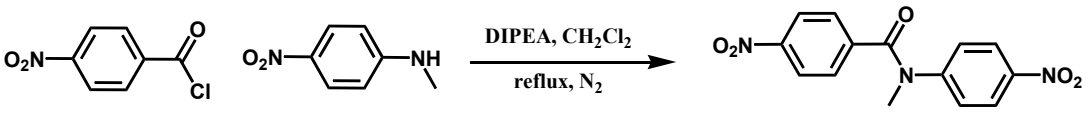

4-Nitrobenzoyl chloride (1.50 g, 8.1 mmol) was dissolved in anhydrous dichloromethane (25 mL). *N,N*-Diisopropylethylamine (2 mL, 1.49 g, 11.6 mmol, 1.4 eq.) was then added under nitrogen and the mixture was cooled to 0 °C. *N*-methyl-4-nitroaniline (1.01 g, 6.6 mmol, 0.8 eq.) was added and the mixture was allowed to warm to room temperature. The mixture was then refluxed under nitrogen and the progression

of the reaction was monitored by TLC analysis (SiO_2, CH_2Cl_2). After 2 hours the mixture was cooled to room temperature and diluted to 50 mL with dichloromethane. The solution was washed successively with 5% aqueous $NaHCO_3$ (2 × 50 mL), 5% aqueous citric acid (2 × 50 mL) and water (1 × 50 mL). The organic layer was collected, dried over Na_2SO_4, filtered and the solvent was evaporated. Column chromatography (SiO_2, elution gradient: CH_2Cl_2 to CH_2Cl_2: 2.5%-EtOAc) yielded the desired compound (second eluted band) as a light yellow solid (1.86 g, 6.2 mmol, 94%).
^{1}H-NMR (400 MHz, $CDCl_3$) δ (ppm): 8.14 (d, *J* = 8.0 Hz, 2H); 8.11 (d, *J* = 8.0 Hz, 2H); 7.50 (d, *J* = 8.0 H, 2H); 7.23 (d, *J* = 8.0 Hz, 2H); 3.58 (s, 3H).
^{13}C-NMR (101 MHz, $CDCl_3$) δ (ppm): 168.23, 149.42, 148.50, 145.72, 141.00, 129.58, 126.91, 124.94, 123.53, 38.21.
HRMAS (m/z): calc for $C_{14}H_{11}N_3O_5$+H^+, 302.07715; found, 302.07720.

_N_-methyl-4-amino-_N_-(4-aminophenyl)benzamide

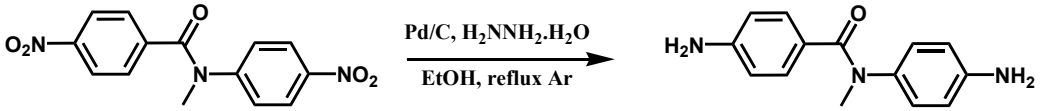

N-Methyl-4-nitro-*N*-(4-nitrophenyl)benzamide (0.5 g, 1.66 mmol) was suspended in absolute ethanol (150 mL). The mixture was then purged with argon (3 vacuum-argon cycles). 5%-palladium on carbon (150 mg) was added and the suspension warmed to 70 °C under argon. Hydrazine monohydrate (1.7 mL, 1.74 g, 35 mmol, 21 eq) was added and the mixture refluxed under argon for 4 hours. TLC analysis (SiO_2, CH_2Cl_2:5%- EtOAc) showed complete conversion. The mixture was cooled to room temperature and the mixture filtered over a short Celite plug. The plug was then washed with ethanol (50 mL) and the solvent evaporated to yield the desired compound as a white solid (380 mg, 1.56 mmol, 95%).
^{1}H-NMR (400 MHz, $CDCl_3$) δ (ppm): 7.16 (d, *J* = 8.5 Hz, 2H), 6.82 (d, *J* = 8.6 Hz, 2H), 6.53 (d, *J* = 8.6 Hz, 2H), 6.41 (d, *J* = 8.6 Hz, 2H), 3.74 (brs, 2H), 3.64 (brs, 2H), 3.39 (s, 3H).
^{13}C-NMR (101 MHz, $CDCl_3$) δ (ppm): 170.47, 147.57, 144.55, 136.83, 130.92, 127.81, 125.69, 115.37, 113.51, 38.86.
HRMAS (m/z): calc for $C_{14}H_{15}N_3O$+H^+, 242.12879; found, 242.12885.

_N_-isopropyl-4-nitro-_N_-(4-nitrophenyl)benzamide

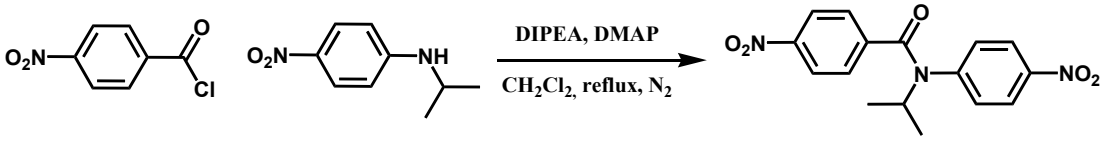

N-Isopropyl-4-nitroaniline (161 mg, 0.89 mmol) was dissolved in anhydrous dichloromethane (20 mL) under nitrogen. *N,N*-Diisopropylethylamine (1 mL, 747 mg, 5.8 mmol, 6.5 eq.) and 4-(N,N-dimethylamino)pyridine (75 mg, 0.7 eq.) were then added, followed by 4-nitro-benzoyl chloride (600 mg, 3.23 mmol, 3,6 eq). The mixture was refluxed under nitrogen and the progression of the reaction followed by TLC analysis (SiO_2, CH_2Cl_2). Following the first 2 hours of reflux, 3 × 200 mg of 4-nitro-benzoyl chloride (total quantity added 600 mg, 3.23 mmol, 3.6 eq) and 3 × 0.33 mL *N,N*-diisopropylethylamine (total quantity added, 1 mL, 747 mg, 5.8 mmol, 6.5 eq.) were added over the course of the 6 hours needed to complete the reaction. The mixture was then cooled to room temperature, diluted to 50 mL with dichloromethane and subsequently successively washed with 5% aqueous $NaHCO_3$ solution (3 × 50 mL),

5% aqueous citric acid solution (3 × 50 mL) and water (1 × 50 mL). The organic layer was collected, dried over Na_2SO_4, filtered and the solvent evaporated. Column chromatography (SiO_2, CH_2Cl_2:0.5%-EtOAc) yielded the desired compound (second eluted band) as a pale yellow solid (220 mg, 0.67 mmol, 75%).
^{1}H-NMR (400 MHz, $CDCl_3$) δ (ppm): 8.12 (d, *J* = 8.9 Hz, 2H), 8.03 (d, *J* = 8.7 Hz, 2H), 7.40 (d, *J* = 8.7 Hz, 2H), 7.19 (d, *J* = 8.8 Hz, 2H), 5.04 (h, *J* = 6.8 Hz, 1H), 1.26 (d, *J* = 6.8 Hz, 6H).
^{13}C-NMR (101 MHz, $CDCl_3$) δ (ppm): 168.06, 148.04, 146.83, 145.11, 142.26, 130.93, 128.95, 124.46, 123.39, 49.28, 21.02.
HRMAS (m/z): calc for $C_{16}H_{15}N_3O_5$+H^+, 330.10845; found, 330.10774.

_N_-isopropyl-4-amino-_N_-(4-aminophenyl)benzamide

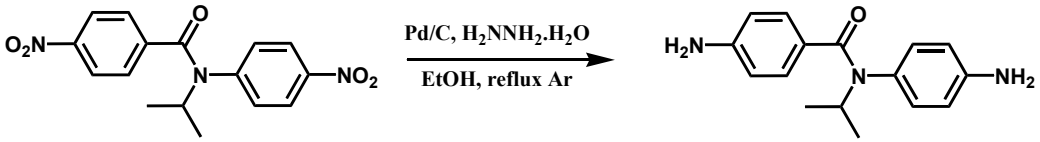

N-Isopropyl-4-nitro-*N*-(4-nitrophenyl)benzamide (200 mg, 0.61 mmol) was suspended in absolute ethanol (75 mL). The mixture was purged with argon (3 vacuum-argon cycles). 5%-palladium on carbon (75 mg) was added and the suspension warmed to 70 °C under argon. Hydrazine monohydrate (0.85 mL, 0.87 g, 17 mmol, 28 eq) was added and the mixture refluxed under argon for 2 hours. TLC analysis (SiO_2, CH_2Cl_2:5%- EtOAc) showed complete conversion. The mixture was cooled to room temperature and filtered over a short Celite plug. The plug was washed with ethanol (30 mL) and the solvent evaporated to yield the desired compound as a white solid (151 mg, 0.56 mmol, 92%).
^{1}H-NMR (400 MHz, $CDCl_3$) δ (ppm): 7.10 (d, *J* = 8.2 Hz, 2H), 6.77 (d, *J* = 8.2 Hz, 2H), 6.51 (d, *J* = 8.2 Hz, 2H), 6.38 (d, *J* = 8.1 Hz, 2H), 5.20 – 4.85 (m, 1H), 3.93 – 3.27 (m, 6H).
^{13}C-NMR (101 MHz, $CDCl_3$) δ (ppm): 170.68, 147.06, 145.23, 131.39, 130.81, 130.36, 127.25, 114.80, 113.53, 47.26, 21.03.
HRMAS (m/z): calc for $C_{16}H_{19}N_3O$+H^+, 270.16009; found, 270.16012.

4-nitro-_N_-(4-nitro-2,5-dimethoxyphenyl)benzamide

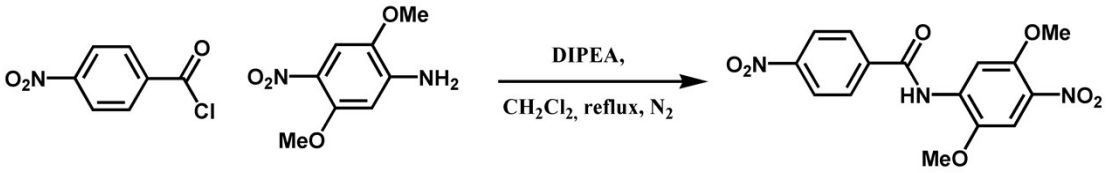

4-Nitrobenzoyl chloride (702 mg, 3.8 mmol) was dissolved in anhydrous dichloromethane (25 mL) under nitrogen. *N,N*-Diisopropylethylamine (0.68 mL, 508 mg, 4 mmol) was added, followed by 4-nitro-2,5-dimethoxyaniline (500 mg, 2.5 mmol), and the mixture refluxed under nitrogen. The reaction was followed by TLC analysis (SiO_2, CH_2Cl_2). After 2 hours of reflux, 4-nitrobenzoyl chloride (150 mg, 0.81 mmol) and *N,N*-diisopropylethylamine (0.15 mL, 113 mg, 0.87 mmol) were added and the mixture was refluxed under nitrogen for a further 2 hours. The reaction mixture was then cooled to room temperature, diluted to 100 mL with dichloromethane, and subsequently successively washed with a 5% aqueous $NaHCO_3$ solution (3 × 50 mL), a 5% aqueous citric acid solution (3 × 50 mL) and water (1 × 50 mL). The organic layer was collected, dried over Na_2SO_4, filtered and the crude mixture was adsorbed

on silica (30 mL). Column chromatography (SiO_2, dry loading, elution gradient $CHCl_3$:1%-EtOAc to $CHCl_3$:2%-EtOAc) yielded the desired compound as a yellow solid (715 mg, 2.05 mmol, 82%).
^{1}H-NMR (400 MHz, DMSO-d_6) δ (ppm): 10.11 (s, 1H), 8.35 (d, J = 8.7 Hz, 2H), 8.15 (d, J = 8.7 Hz, 2H), 8.03 (s, 1H), 7.66 (s, 1H), 3.88 (s, 6H).
^{13}C-NMR (101 MHz, DMSO-d_6) δ (ppm): 164.79, 149.85, 147.63, 144.31, 140.04, 134.78, 133.21, 129.84, 124.06, 109.11, 108.73, 57.38, 57.18.
HRMAS (m/z): calc for $C_{15}H_{13}N_3O_7$+H^+, 348.08263; found, 348.08238.

4-amino-*N*-(4-amino-2,5-dimethoxyphenyl)benzamide

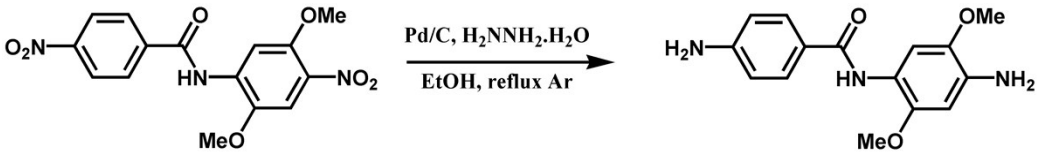

4-Nitro-*N*-(4-nitro-2,5-dimethoxyphenyl)benzamide (250 mg, 0.72 mmol) was suspended in absolute ethanol (75 mL). The mixture was purged with argon (3 vacuum-argon cycles). 5%-palladium on carbon (75 mg) was added and the suspension warmed to 70 °C under argon. Hydrazine monohydrate (0.85 mL, 0.87 g, 17 mmol, 24 eq) was added and the mixture refluxed under argon for 2 hours. TLC analysis (SiO_2, CH_2Cl_2:10%- EtOAc) showed complete conversion. The mixture was cooled to room temperature and filtered over a short Celite plug. The plug was washed with ethanol (50 mL) and the solvent was evaporated to yield the desired compound as a slightly off-white solid (167 mg, 0.58 mmol, 81%).
^{1}H-NMR (400 MHz, DMSO-d_6) δ (ppm): 8.66 (s, 1H), 7.62 (d, J = 8.5 Hz, 2H), 7.20 (s, 1H), 6.55 (d, J = 8.5 Hz, 2H), 6.40 (s, 1H), 5.64 (s, 2H), 4.63 (s, 2H), 3.67 (s, 6H).
^{13}C-NMR (101 MHz, DMSO-d_6) δ (ppm): 164.95, 152.21, 146.72, 139.82, 135.59, 129.23, 121.72, 116.16, 113.09, 109.64, 99.18, 56.42, 56.34.
HRMAS (m/z): calc for $C_{15}H_{17}N_3O_3^+$, 287.12699; found, 287.12666.

Computational Details

Description of the Leads:

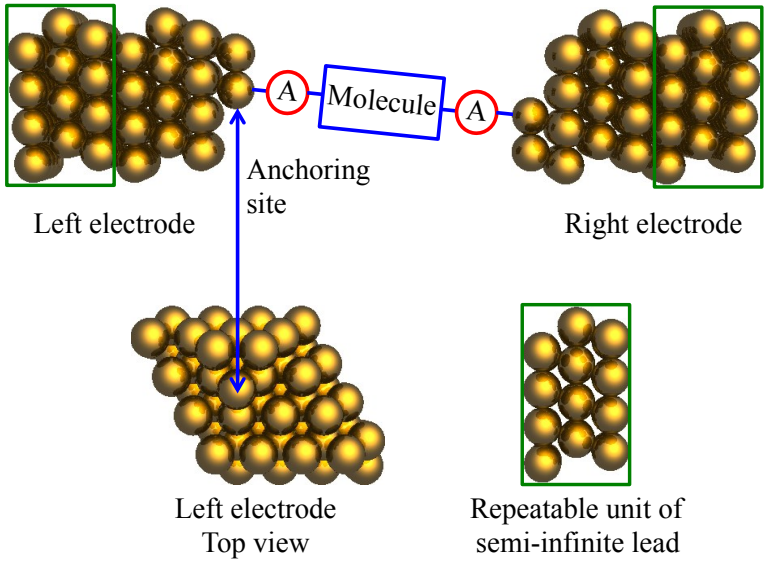

Figure S1. The electrodes used for extended systems in *I-V* curve calculations. They consist of 6 layers of 16 gold atoms cut from an Au fcc lattice, with a triad contact motif attached to the (111) surface. The lattice constant is 4.080 Å.

Computational Methods:

The molecules analyzed in Table 2 were optimized at the DFT/B3LYP level using 6-311+G(d,p) basis set as implemented in Gaussian 09 v.C01.[1] The isolated molecule used for transport calculations were optimized in gas phase with DFT/B3LYP level using 6-31++G(d,p) basis set. The molecular junctions were prepared by inserting the molecules in between the two gold leads as shown in Figure S1, attaching through the amine terminal groups. I-V curves were obtained by using the DFT-NEGF approach as implemented in the TranSIESTA computational package.[2] The generalized gradient approximation (GGA) functional PBE[3] was used for the calculations with single-ζ basis set for gold atoms and double-ζ basis set for non-gold atoms as implemented in TranSIESTA.[2] A Monkhorst-Pack k-point grid of 10×10×80 was used to sample the Brillouin zone for the gold electrode and a grid of 10×10×1 for the molecular region. The energy cutoff for the real space grid was set to 200 Ry.

Single-State Tight-binding (TB) Model:

For computational efficiency and from earlier experience,[4-7] all screening calculations in our recent study[8] were performed with the nanowire leads and the thiolate anchoring groups. However, amine anchoring groups are found to form a better linkage between molecules and scanning tunneling microscope (STM) tips. Hence, we developed a method that enables us to computationally probe the *I-V* characteristics of molecules with amine anchoring groups that were identified by our screening process. Therefore, results from the screening process should be only able to predict trends in rectification ratio (RR) as a function of molecular structure but may not accurately predict the absolute value for the RR. For this reason, once the screening process is finished, the most promising candidates are selected for a subsequent refining step, in order to obtain an accurate absolute rectification ratio using a more realistic model.

Previous studies[9, 10] have shown that the low-bias molecular rectification is due to the shifting of the transport state (a frontier molecular orbital, i.e. HOMO or LUMO) closest to the Fermi level under the applied bias. Therefore, we can use the single-state tight-binding model for a more realistic calculation for molecules with anchoring groups other than thiolate groups. In this model, the molecule is approximated as one single state, connected to two leads in a tight-binding fashion. For such a system, the transmission function as a function of energy, ε, under a particular applied bias, V, can be described by the Breit-Wigner formula:[11]

$$T(\varepsilon, \mathrm{V}) = \frac{4\Lambda_L \Lambda_R}{[\varepsilon - \varepsilon_0(\mathrm{V})]^2 + (\Lambda_L + \Lambda_R)^2} \quad (1)$$

where ε_0 is the energy of the isolated state, and Λ_L and Λ_R are the coupling to the left and right electrodes, respectively. According to this model, rectification is caused only by asymmetric shifting of ε_0 with respect to the applied bias. Hence, we are assuming that the overall shape of the transmission function will not be affected under low bias.

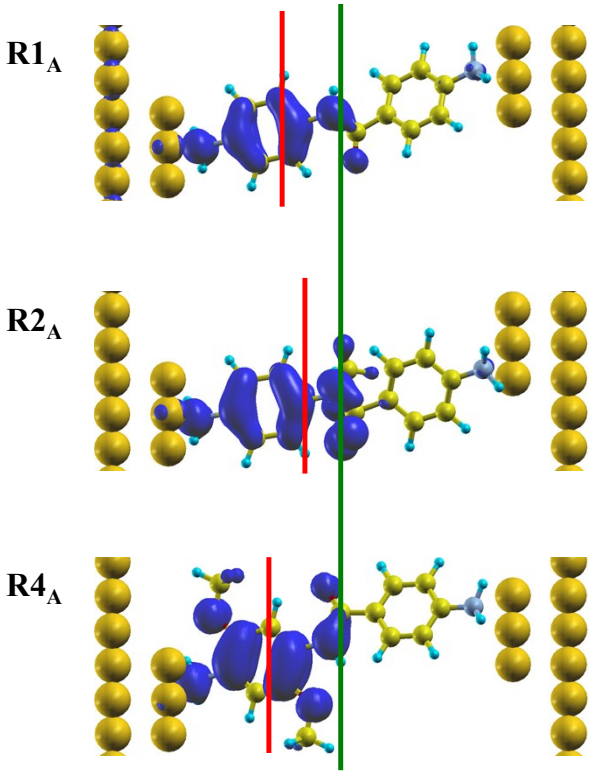

Figure S2. The LDOS for **R1**$_A$, **R2**$_A$, and **R4**$_A$. The green line indicates the center point in the transport direction of the junction (between the gold leads). The red lines indicate the "center of mass" of the conducting molecular states in the transport direction for each molecule.

Our single state ε_0 will be spatially localized at the "center of mass" of the conducting molecular state (or gateway orbital) shown in Figure S2. In the case of the present work we have determined that the HOMO of the molecule is the primary orbital responsible for the electronic conductance, and its "center of mass" will determine the position of the single state. With the present molecular orientation, the HOMO is localized on the 4-carboxy-aniline side of the molecule (see **Figure S2**). Accordingly, when a positive bias is applied, ε_0 increases as the value of applied bias increases, and decreases as the bias decreases.[10] It is assumed that the bias experienced by the molecule is linearly decreasing from the molecule-lead contact point to the geometric center of the junction. Hence, the change of ε_0 is proportional to distance in the transport direction between the HOMO "center of mass" and closest contact point:

$$\varepsilon_0(\mathrm{V}) = \varepsilon_0(0) + \mathrm{V} \times \frac{\text{state - lead distance}}{\text{junction length}} \tag{2}$$

where V is the applied bias. Therefore, the transmission function under different bias can be approximated by substituting Eq. (2) into Eq. (1):

$$T(\varepsilon, \mathrm{V}) = \frac{4\Lambda_L \Lambda_R}{\left\{\varepsilon - \left[\varepsilon_0(0) + \mathrm{V} \times \frac{\text{state - lead distance}}{\text{junction length}}\right]\right\}^2 + (\Lambda_L + \Lambda_R)^2} \tag{3}$$

Assuming that the shape of transmission function does not change under low bias, $\varepsilon_0(0)$, Λ_L, and Λ_R can be obtained by fitting the dominant transmission peak using Eq. (3), treating these three quantities as parameters, and setting V to 0. Meanwhile, the spatial position of $\varepsilon_0(0)$ can be approximated by using the coordinates of the center of mass of the HOMO. The state-lead distance is the distance between the molecule-lead contact point and the center of mass of the HOMO, projected onto the transport direction. Once all the parameters are obtained, the transmission function of the dominant transport state under different biases can be calculated, and in turn the current under those biases is computed.

Table S1. Parameters from zero-bias transmission function fitted by Eq. (4). Units are eV.

Molecule	$\varepsilon_0(0)$	Λ_L	Λ_R
$\mathbf{R1_A}$	-1.661	-0.0447	-0.0034
$\mathbf{R2_A}$	-1.580	-0.0298	-0.0008
$\mathbf{R4_A}$	-1.091	-0.0406	-0.0010

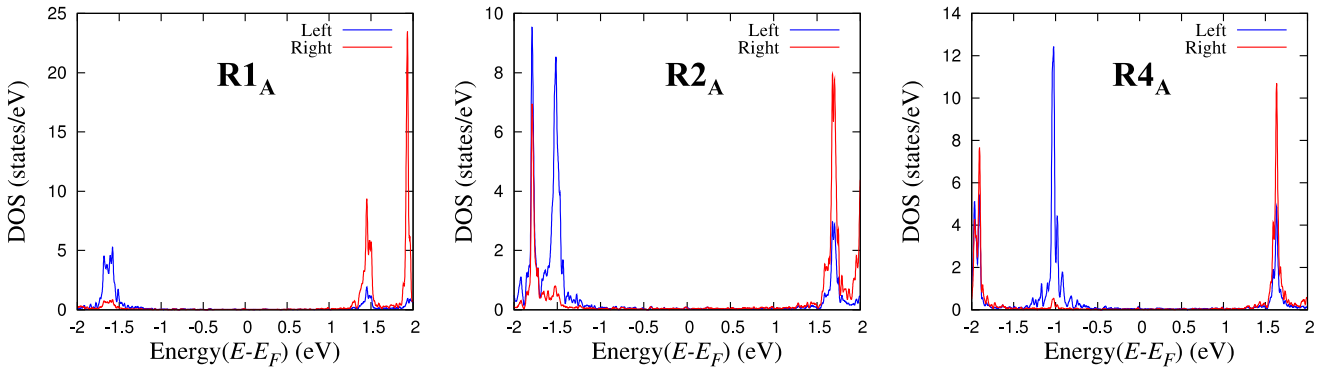

Figure S3. Density of states for molecules $\mathbf{R1_A}$, $\mathbf{R2_A}$, and $\mathbf{R4_A}$. "Left" in legends means electron density of the HOMO localized on the 4-carboxy-aniline group, while "Right" means localization on the phenyldiamine group.

References

1. M. J. Frisch, G. W. Trucks, H. B. Schlegel, G. E. Scuseria, M. A. Robb, J. R. Cheeseman, G. Scalmani, V. Barone, B. Mennucci, G. A. Petersson, H. Nakatsuji, M. Caricato, X. Li, H. P. Hratchian, A. F. Izmaylov, J. Bloino, G. Zheng, J. L. Sonnenberg, M. Hada, M. Ehara, K. Toyota, R. Fukuda, J. Hasegawa, M. Ishida, T. Nakajima, Y. Honda, O. Kitao, H. Nakai, T. Vreven, J. Montgomery, J. A., J. E. Peralta, F. Ogliaro, M. Bearpark, J. J. Heyd, E. Brothers, K. N. Kudin, V. N. Staroverov, R. Kobayashi, J. Normand, K. Raghavachari, A. Rendell, J. C. Burant, S. S. Iyengar, J. Tomasi, M. Cossi, N. Rega, J. M. Millam, M. Klene, J. E. Knox, J. B. Cross, V. Bakken, C. Adamo, J. Jaramillo, R. Gomperts, R. E. Stratmann, O. Yazyev, A. J. Austin, R. Cammi, C. Pomelli, J. W. Ochterski, R. L. Martin, K. Morokuma, V. G. Zakrzewski, G. A. Voth, P. Salvador, J. J. Dannenberg, S. Dapprich, A. D. Daniels, Ö. Farkas, J. B. Foresman, J. V. Ortiz, J. Cioslowski and D. J. Fox, *Journal*, 2009, **Revision A.1**.
2. M. Brandbyge, J.-L. Mozos, P. Ordejón, J. Taylor and K. Stokbro, *Phys. Rev. B*, 2002, **65**, 165401.
3. J. P. Perdew, K. Burke and M. Ernzerhof, *Phys. Rev. Lett.*, 1996, **77**, 3865-3868.
4. B. Xu and N. J. Tao, *Science*, 2003, **301**, 1221-1223.
5. C. Li, I. Pobelov, T. Wandlowski, A. Bagrets, A. Arnold and F. Evers, *J. Am. Chem. Soc.*, 2008, **130**, 318-326.
6. A. Mishchenko, D. Vonlanthen, V. Meded, M. Bürkle, C. Li, I. V. Pobelov, A. Bagrets, J. K. Viljas, F. Pauly, F. Evers, M. Mayor and T. Wandlowski, *Nano Lett.*, 2010, **10**, 156-163.
7. C. Bruot, L. Xiang, J. L. Palma and N. Tao, *ACS Nano*, 2015, **9**, 88-94.
8. W. Ding, M. Koepf, C. Koenigsmann, A. Batra, L. Venkataraman, C. F. A. Negre, G. W. Brudvig, R. H. Crabtree, C. A. Schmuttenmaer and V. S. Batista, *J. Chem. Theory Comput.*, 2015, **11**, 5888-5896.
9. W. Ding, C. F. A. Negre, J. L. Palma, A. C. Durrell, L. J. Allen, K. J. Young, R. L. Milot, C. A. Schmuttenmaer, G. W. Brudvig, R. H. Crabtree and V. S. Batista, *ChemPhysChem*, 2014, **15**, 1138-1147.
10. W. Ding, C. F. A. Negre, L. Vogt and V. S. Batista, *J. Chem. Theory Comput.*, 2014, **10**, 3393-3400.
11. J. C. Cuevas and E. Scheer, *Molecular Electronics: An Introduction to Theory and Experiment*, World Scientific Publishers, 2010.